

High-Entropy Alloy Coatings: State and Prospects

V. E. Gromov^{a,*} (ORCID: 0000-0002-5147-5343), S. V. Konovalov^{a,**} (ORCID: 0000-0003-4809-8660),
O. A. Peregudov^{b,***} (ORCID: 0000-0001-5154-5498), M. O. Efimov^{a,****} (ORCID: 0000-0002-4890-3730),
and Yu. A. Shlyarova^{a,*****} (ORCID: 0000-0001-5677-1427)

^a Siberian State Industrial University, Novokuznetsk, 654007 Russia

^b Omsk State University, Omsk, 644050 Russia

*e-mail: gromov@physics.sibsiu.ru

**e-mail: ksv@ssau.ru

***e-mail: olegomgtu@mail.ru

****e-mail: moefimov@mail.ru

*****e-mail: rubannikova96@mail.ru

Received August 30, 2022; revised September 9, 2022; accepted September 9, 2022

Abstract—We have made a brief review of recent foreign and domestic publications, in which the structures, phase compositions, and properties of films and coatings of five-component high-entropy alloys (HEA) on different substrates and the modification of HEA surfaces by different kinds of treatment have been studied. The main methods of film deposition and coatings such as magnetron sputtering, thermal evaporation, laser deposition, and electrodeposition are discussed in the paper. Special attention is paid to the deposition of coatings on stainless steels and titanium alloys. A positive change in the tribological, strength properties, and corrosion resistance of film coatings is seen in a wide temperature range. Possible reasons for the observed effects are discussed considering the role of solid-solution hardening, the formation of a fine-grained structure, and the formation of oxide layers enriched by one of the HEA components. New methods for deposition of HEA coatings and subsequent treatment have been distinguished. The role of niobium and titanium in an increase in the microhardness, wear resistance, and decrease in the friction coefficient of the coatings is considered exemplified by alloying with these elements. The electrolytic polishing, electroerosive machining, mechanical polishing, and combinations thereof are used among the HEA surface treatment methods. In some works, it is suggested to use the powder boriding technique to increase the surface strength and wear resistance of HEA. The studies have been analyzed with respect to electron-beam treatment—one of the promising and highly effective methods of HEA surface hardening.

Keywords: coatings, films, high-entropy alloys, deposition methods, tribological properties, mechanical properties, wear resistance

DOI: 10.3103/S0967091222100047

INTRODUCTION

High-entropy alloys (HEA) are a new class of materials that consist of at least five elements in the equiatomic or close to equiatomic ratio, which provides them, unlike traditional alloys, with unique properties [1]. The concept of HEA is based on the idea that a high mixing entropy can promote the formation of stable single-phase microstructures [2], which does not contradict the phase rule based on the laws of thermodynamics. There is an unprecedented worldwide interest in the development and research of HEAs. The first work in this direction should be considered study [3], in which the atomic concentration of the elements that compose the HEA ranges from 5 to 35%. The features of the chemical composition and structure of HEA lead to the so-called core effects, which determine the unique properties of these mate-

rials [4–7]: the effect of high entropy, the effect of strong distortions of a crystal lattice, the effect of delayed diffusion and the cocktail effect. The first effect is that a decrease in the entropy upon transition to a more ordered state outweighs the decrease in enthalpy due to the effect of the formation of an ordered phase [2, 8]. The effect of crystal lattice distortions is due to the fact that atoms with different sizes randomly occupy interstices in the crystal lattice. Obviously, larger atoms will be located at the maximum distance from each other since in this case the distortions of the crystal structure and the system energy will decrease. The effect of delayed diffusion is associated with the effect of distortions of the crystal lattice as well as with the formation of nanosized inclusions and amorphous multicomponent phases in different methods of obtaining HEA [2, 9–12]. This

effect is of great practical importance since, e.g., the corrosion resistance depends on the diffusion rate. There is no strict definition of the cocktail effect; it usually means the ability of an alloy to have properties that are inaccessible to each of its components separately [2, 4]. As a rule, the HEA has properties that exceed the summed properties of all the alloy components.

The extensive original results, comments, analysis of the HEA properties, and prospects for HEA application are generalized in reviews and monographs [1, 15, 16]. In publications [17, 18], a brief review of recent foreign researches of the structural and basic states and properties of five-component high-entropy alloys over a wide temperature range is carried out. Among the works of domestic researchers for the previous five years, publications [19–24] should be noted, in which the effect of composition on the mechanical properties and fine structure parameters of single- and polycrystalline HEAs obtained by different methods was studied.

In last five years, despite many publications on HEA and the existing serious problems analyzed in [1, 2, 15, 16], two fundamentally new directions in the physics of HEA have emerged: improving surface properties by fabrication of thin coatings and films; modification of the HEA surface by different treatment processes.

RESULTS AND DISCUSSION

Among many methods for deposition of HEA films or coatings, it is necessary to focus on four of them, which have a number of advantages: magnetron sputtering [25], thermal evaporation [26], laser evaporation [27, 28], and electrodeposition [29]. The use of HEA coatings instead of bulk coatings, on the one hand, substantially reduces the cost of products; on the other hand, substantially expands the scope [29].

Magnetron Sputtering

The first works were carried out to obtain coatings from multicomponent carbides, nitrides, and oxides [30–33]. Recently, multilayer nanostructured laminates have been obtained by magnetron sputtering [34, 35]. It is necessary to focus on a new method to obtain HEA nanoparticles coated with multilayer graphene [36], which can be useful in the mechanical synthesis of HEAs.

Magnetron sputtering of HEA makes it possible to obtain highly uniform thin coatings, the properties of which are substantially better than the substrate properties. Thus, the deposition of a CrNbTiMoZv HEA film by DC magnetron sputtering on 304 stainless steel (International Classification) provides a nano-hardness of 9.7 GPa and excellent tribological properties [37]. The tests of the coating obtained by magnetron sputtering of five AlTiCrNiTa targets on X80 steel demonstrated the chloride corrosion resistance and

density of the film–substrate system [38] during operation. In [39], the corrosion resistance of films based on AlCrTiV with the addition of copper, molybdenum and Cu/Mo additives deposited by magnetron sputtering on 304 stainless steel have been analyzed, and it is substantiated that all the coatings have properties that are substantially superior to those of the substrate due to the formation of stable Al_2O_3 , Cr_2O_3 oxides and others.

Laser Coatings

There are much more publications devoted to the laser method of coating deposition than to the magnetron one. HEA FeNiCoCrMo_x films ($x = 0; 0.15; 0.20; 0.25$) deposited on 304 and 316 stainless steels led to an increase in the microhardness by 90.5% with respect to the substrate and a decrease in the wear rate by 38.9%. A decrease in the friction coefficient and an increase in the corrosion resistance are due, in authors' opinion, to the effect of MeO_3 oxide on the passivating coating [39]. 304 stainless steel coated with different HEAs is a subject of the extensive research [40–44]. The study of AlCoCrFeNi, AlCoCrFeMo, and FeCoCrMnTi coatings [45] shows a positive change in the tribological and strength properties of film coatings and in the corrosion resistance. To counteract high-temperature wear, where the main mechanisms are oxidation and abrasive wear, the authors of [46] suggest to use AlCrFeMnNi HEA coatings that have a protective effect due to the formation of an oxide protective film, which substantially reduces the friction coefficient and the wear parameter up to 0.48 and $1.25 \times 10^{-4} \text{ mm}^3/(\text{N m})$, respectively, at 400°C. The laser exposure, which ensures the re-melting of the surface of Cr13 steel hardened with a high-entropy FeCrCoAl_x coating, leads to the uniform distribution of elements in the body-centered lattice due to the increased mixing entropy and the formation of AlO_x and CrO_x oxide films. All this provides the substantially increased corrosion resistance [47]. The CoCrFeMnTi_{0.2} HEA two-layer coating formed on 15CrMn steel has a microhardness of 428.26 HV0.3, which is 3.5 times higher than that of bulk CoCrFeMnNi HEA. This is obtained due to the solid solution strengthening, precipitation hardening, and martensitic transformation. The wear mechanisms are abrasive and oxidative; the corrosion rate is 0.131 $\mu\text{m}/\text{year}$. Here, the main role belongs to the multigrain coating structure and the presence of highly passivating elements [48].

The introduction of alloying elements into the HEA substantially affects the structural-phase state and properties of the five-component alloy coatings [49]. The FeNiCoCrTi0.5Nb_x ($x = 0.25; 0.50; 0.75; 1.00$) high-entropy alloy contains bcc, fcc, and Laves phases. The upper and lower coating parts are represented by the equiaxed and columnar crystals, and the core contains dendrites with different shapes and a structure in the form of stripes. The hardness of all the

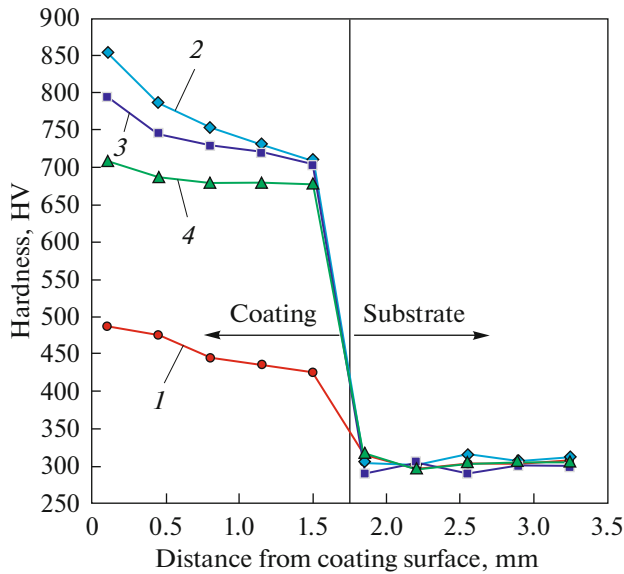


Fig. 1. Change in the hardness of FeNiCoCrTi_{0.5}Nb_x coating as a function of depth at different x [49]: (1) 0.25; (2) 0.50; (3) 0.75; (4) 1.00.

coatings is substantially higher than that of the matrix, and the highest value of 852.5 HV (2.9 times higher than the hardness of matrix) is registered for the FeNiCoCrTi_{0.5}Nb_{0.5} coating (Fig. 1). It also has the lowest rate of abrasive wear.

During the deposition of FeCoNiCrMnTi_x ($x = 0; 0.5; 1.0; 1.5$) HEA coating on 30U stainless steel, TiN reinforcing particles are formed, which are responsible for the improved mechanical and tribological properties [50]. With an increase in the titanium content, the wear resistance, microhardness (Fig. 2), and corrosion resistance increase, while the friction coefficient decreases.

In the aerospace industry, the titanium alloys such as Ti–6Al–4V are widely used but they have many disadvantages, in particular, low wear resistance, hardness, and resistance to chloride corrosion. This is largely eliminated by laser deposition of HEA coatings [51], which have an excellent bond with the Ti–6Al–4V substrate and provide surface hardness and corrosion resistance. The TiZrAlNbCo HEA coating provides a hardness of 768.9 HV and excellent corrosion resistance ($I_{\text{corr}} = 3.66 \times 10^{-9}$ A/cm²). This is due to the formation of fcc phase. The widespread use of the CoCrFeNiMo_{0.2} coating, which consists of a bcc structure with σ -phases and has a uniform dendritic structure, is due to its high (~900 HV0.1) hardness, which is 2.3 times higher than that of the substrate. At 600°C, this coating has good wear resistance [52]. The improved surface properties are due to the combined contribution of solid solution strengthening and fine grain structure as well as to the presence of chromium-rich oxide layers.

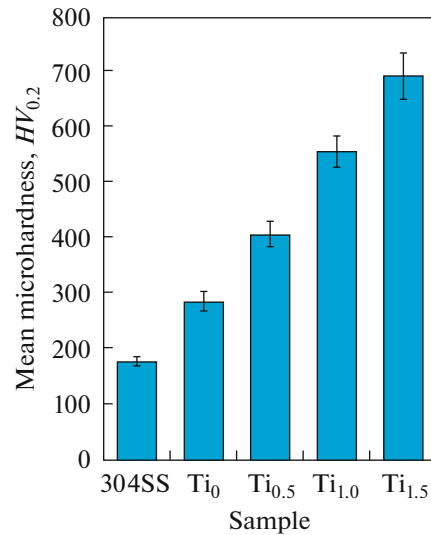


Fig. 2. Dependence of microhardness of FeCoNiCrMnTi_x HEA coating on the titanium content [50].

Among the new methods of deposition of HEA coatings and subsequent treatment, we should focus on paper [53], which analyzes the results of studies of the microstructure, phase composition, grain orientation, and surface morphology of NiFeCrNbTiAl HEA coatings formed by the deposition of supersonic particles followed by laser irradiation. The schematics of supersonic deposition of particles and technological parameters are shown in Fig. 3. The laser irradiation power was 800 W. Argon was used for oxidation protection during the laser processing. This combined technology provided the following product parameters: fatigue limit of 252 MPa, tensile strength of 3000 MPa, relative elongation of 14%, friction coefficient of 0.189, microhardness of 72 GPa, and residual stress of 14.3 MPa. These indicators are provided by the isotropic submicro- and nanosized grain structure.

In order to improve the surface properties, the HEA is subjected to different types of surface treatment. For example, the different treatment methods and their effect on the surface of CoCrFeMnNi HEA obtained by the selective laser melting were reviewed in [54]. The following types of treatment were considered: electrolytic polishing, electroerosive machining, milling, grinding, mechanical polishing using abrasives as well as a combination of those methods. The results demonstrated that the grinding resulted in a smoother surface and an increase in the microhardness; however, it leaves traces from tool action and residual stresses that arise due to the microstructure deformation. The mechanical polishing with abrasives resulted in the ultra-smooth surface with no subsurface damage. The electroerosive machining caused surface melting, which led to an increase in the residual stresses and microhardness. The use of electropo-

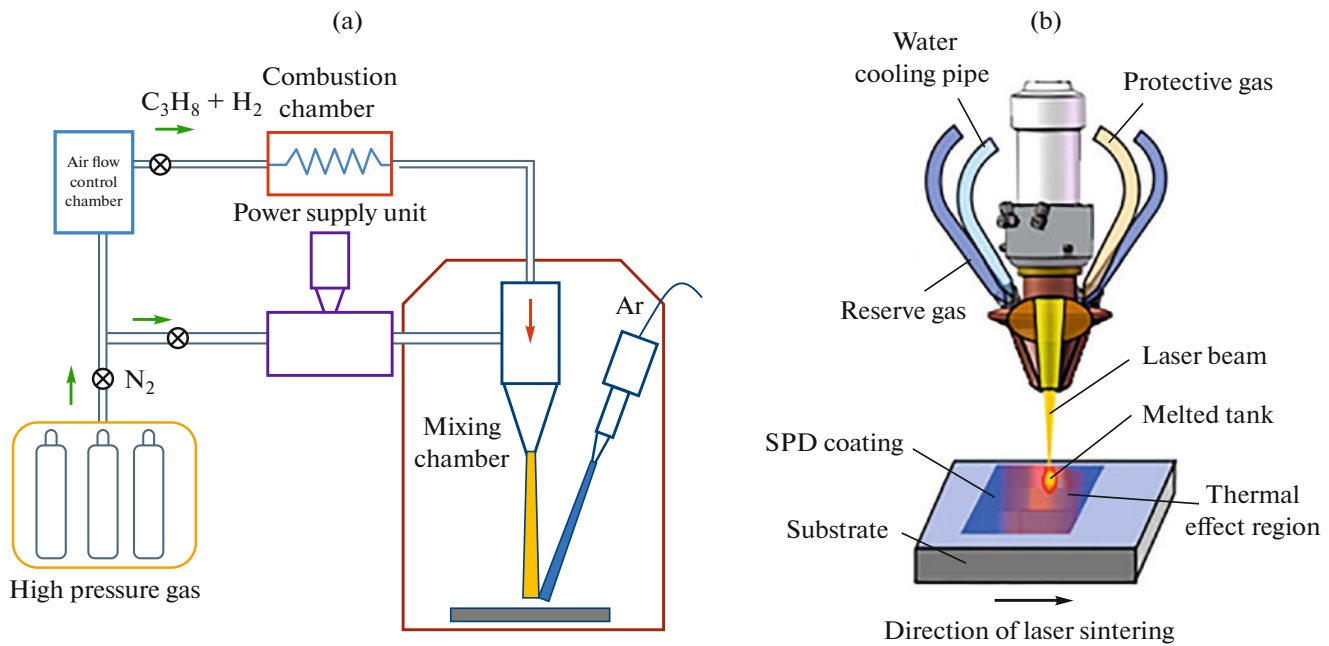


Fig. 3. Systems of supersonic deposition (SPD) (a) of particles and laser irradiation (LI) (b) [53].

lishing in combination with other methods smoothed the surface by means of removing residual stresses and damage from previous processing. However, the use of only electropolishing did not result in the micrometer-level surface roughness. In [55], the problem of low strength and wear resistance of the CoCrFeMnNi alloy with an fcc crystal lattice was solved by the powder-pack boriding. As a result, a double layer enriched with silicon and boron was formed. An increase in the microhardness and wear resistance of borated samples has been established. The similar steps were taken in [56], in which the improvement of density, microstructure, surface perfection, and mechanical properties was obtained by the boriding with CoCrFeNiAl_{0.25} HEA obtained by powder metallurgy at temperatures of 900–1200°C.

In comparison with the initial HEA (47.07 GPa), the elastic modulus increased up to 140–151 GPa, and the impact strength increased up to 3.57–4.25 MPa m^{1/2}. One of the most promising and highly effective methods of surface hardening of products is the electron beam treatment. This treatment provides ultra-high (up to 10⁶ K/s) heating rates of the surface layer to given temperatures and cooling of the surface layer due to heat removal mainly into material bulk at rates of 10⁴–10⁹ K/s, as a result of which nonequilibrium submicro- and nanocrystalline structural and phase states are formed in the surface layer [57, 58].

Papers [59–63] present the analysis of the structural-phase states and properties of CrMnFeCoNi and CoCrFeNiAl HEAs of non-equiatomic compositions obtained by the wire-arc additive manufacturing

(WAAM) and subjected to electron-beam treatment (EBT) with the following parameters: energy density of the electron beam of 10–30 J/cm², duration of 50–200 μs, frequency of 0.3 s⁻¹, number of pulses of 3. It is shown that the EBT that leads to the high-speed crystallization of a molten surface layer is accompanied by the formation of a nanocrystalline columnar structure, increases the strength and plastic properties of HEA, and homogenizes the material.

The irradiation of the Cantor alloy with electron beams with an energy density of 10–30 J/cm², a duration of 50 μs, a frequency of 0.3 s⁻¹, and a number of pulses of 3 does not lead to a change in the elemental composition; however, it substantially transforms the defective substructure. First, it leads to a substantial (six times, from 20 to 120 μm) increase in the mean grain size; secondly, to the formation of a structure of high-speed cellular crystallization with a cell size of 400–550 nm in the a surface layer approximately 5 μm thick; thirdly, to the formation of a high-speed crystallization texture of the molten surface layer. It is shown that the irradiation with a pulsed electron beam leads to the formation of a gradient dislocation substructure (Fig. 4). A non-disoriented cellular dislocation substructure is formed in the surface layer, in bulk cells of which randomly distributed dislocations are observed. At a depth of 25 μm a non-disoriented cellular-net dislocation substructure is formed with the highest dislocation density of 5.5 × 10¹⁰ cm⁻². Alongside with a cellular-net dislocation substructure, there is a structure formed by the randomly distributed dislocations at a depth of 45 μm. The viscous character of

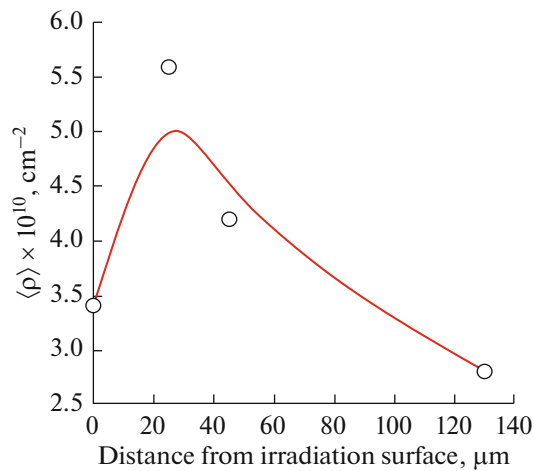


Fig. 4. Dependence of scalar dislocation density on the distance from the irradiation surface of Co–Cr–Fe–Mn–Ni HEA system ($E_s = 20 \text{ J/cm}^2$).

HEA destruction and the formation of regions with a lamellar structure after the EBT were revealed [64].

CONCLUSIONS

The studies on high-entropy alloys films and coatings and surface modification by different methods are substantially intensified for the last five years. The papers on the methods of deposition of coatings on stainless steels and titanium alloys, which improve tribological and mechanical properties, and corrosion resistance over a wide temperature range, are reviewed and analyzed. The attention is focused on the analysis of physical mechanisms of the observed effects. New aspects of coating deposition and post-treatment are considered. The potentials for the use of electron-beam treatment to modify and harden the HEA surface are shown.

FUNDING

The work was supported by the Russian Science Foundation, project no. 20-19-00452.

CONFLICT OF INTEREST

The authors declare that they have no conflicts of interest.

REFERENCES

- Gromov, V., Kononov, S.V., Ivanov, Yu.F., and Osintsev, K.A., *Structure and Properties of High-Entropy Alloys*, Advanced Structured Materials, vol. 107, Cham: Springer, 2021. <https://doi.org/10.1007/978-3-030-78364-8>
- Rogachev, A.S., Structure, stability and properties of high-entropy alloys, *Phys. Met. Metallogr.*, 2020,

vol. 121, no. 8, pp. 733–764.

<https://doi.org/10.1134/S0031918X20080098>

- Yeh, J.-W., Chen, S.-K., Lin, S.-J., Gan, J.-Y., Chin, T.-S., Shun, T.-T., Tsau, C.-H., and Chang, S.-Y., Nanostructured high entropy alloys with multiple principal elements: Novel alloy design concepts and outcomes, *Adv. Eng. Mater.*, 2004, vol. 6, no. 5, pp. 299–303. <https://doi.org/10.1002/adem.200300567>
- Zhang, Y., Zuo, T.T., Tang, Z., Gao, M.C., Dahmen, K.A., Liaw, P.K., and Lu, Z.P., Microstructures and properties of high-entropy alloys, *Prog. Mater. Sci.*, 2014, vol. 61, pp. 1–93. <https://doi.org/10.1016/j.pmatsci.2013.10.001>
- Cantor, B., Multicomponent and high entropy alloys, *Entropy*, 2014, vol. 16, no. 9, pp. 4749–4768. <https://doi.org/10.3390/e16094749>
- Miracle, D.B. and Senkov, O.N., A critical review of high entropy alloys and related concepts, *Acta Mater.*, 2017, vol. 122, pp. 448–511. <https://doi.org/10.1016/j.actamat.2016.08.081>
- Zhang, W., Liaw, P.K., and Zhang, Y., Science and technology in high-entropy alloys, *Sci. China Mater.*, 2018, vol. 61, no. 1, pp. 2–22. <https://doi.org/10.1007/s40843-017-9195-8>
- Gorban', V.F., Krapivka, N.A., and Firstov, S.A., High-entropy alloys: Interrelations between electron concentration, phase composition, lattice parameter, and properties, *Phys. Met. Metallogr.*, 2017, vol. 118, no. 10, pp. 970–981. <https://doi.org/10.1134/S0031918X17080051>
- Yeh, J.-W., Chen, S.-K., Gan, J.-Y., Lin, S.-J., Chin, T.-S., Shun, T.-T., Tsau, C.-H., and Chang, S.-Y., Formation of simple crystal structures in Cu–Co–Ni–Cr–Al–Fe–Ti–V alloys with multiprincipal metallic elements, *Metall. Mater. Trans. A*, 2004, vol. 35, pp. 2533–2536. <https://doi.org/10.1007/s11661-006-0234-4>
- Yeh, J.-W., Recent progress in high-entropy alloys, *Ann. Chim.: Sci. Mater.*, 2006, vol. 31, no. 6, pp. 633–648. <https://doi.org/10.3166/acsm.31.633-648>
- Tong, C.J., Chen, Y.-L., Chen, S.-K., Yeh, J.-W., Shun, T.-T., Tsau, C.-H., Lin, S.-J., and Chang, S.-Y., Microstructure characterization of Al_xCoCrCuFeNi high-entropy alloy system with multi-principal elements, *Metall. Mater. Trans. A*, 2004, vol. 36, pp. 881–893. <https://doi.org/10.1007/s11661-005-0283-0>
- Tsai, K.-Y., Tsai, M.-H., and Yeh, J.-W., Sluggish diffusion in Co–Cr–Fe–Mn–Ni high-entropy alloys, *Acta Mater.*, 2013, vol. 61, no. 13, pp. 4887–4897. <https://doi.org/10.1016/j.actamat.2013.04.058>
- Tsai, M.-H. and Yeh, J.-W., High-entropy alloys: A critical review, *Mater. Res. Lett.*, 2014, vol. 2, no. 3, pp. 107–123. <https://doi.org/10.1080/21663831.2014.912690>
- Alaneme, K.K., Bodunrin, M.O., and Oke, S.R., Processing, alloy composition and phase transition effect on the mechanical and corrosion properties of high entropy alloys: A review, *J. Mater. Res. Technol.*, 2016,

- vol. 5, no. 4, pp. 384–393.
<https://doi.org/10.1016/j.jmrt.2016.03.004>
15. Murty, B.S., Yeh, J.-W., Ranganathan, S., and Bhat-tacharjee, P.P., *High-Entropy Alloys*, Amsterdam: Elsevier, 2019, 2nd ed.
 16. Zhang, Y., *High-Entropy Materials: A Brief Introduction*, Singapore: Springer, 2019.
<https://doi.org/10.1007/978-981-13-8526-1>
 17. Osintsev, K.A., Gromov, V.E., Konovalov, S.V., Ivanov, Yu.F., and Panchenko, I.A., High-entropy alloys: Structure, mechanical properties, deformation mechanisms and applications, *Steel Transl.*, 2022, vol. 52, no. 2, pp. 167–173.
<https://doi.org/10.3103/S0967091222020176>
 18. Gromov, V.E., Rubannikova, Yu.A., Konovalov, S.V., Osintsev, K.A., and Vorob'ev, S.V., Generation of increased mechanical properties of Cantor high-entropy alloy, *Izv. Vyssh. Uchebn. Zaved. Chern. Metall.*, 2021, vol. 64, no. 8, pp. 599–605.
<https://doi.org/10.17073/0368-0797-2021-8-599-605>
 19. Gorbachev, I.I., Popov, V.V., Kats-Dem'yanets, A., Popov, M.L., and Eshed, E., Prediction of the phase composition of high-entropy alloys based on Cr–Nb–Ti–V–Zr using the Calphad method, *Phys. Met. Metallogr.*, 2019, vol. 120, no. 4, pp. 378–386.
<https://doi.org/10.1134/S0031918X19040069>
 20. Gorban', V.F., Krapivka, N.A., Firstov, S.A., and Kurilenko, D.V., Role of various parameters in the formation of the physicochemical properties of high-entropy alloys with BCC lattices, *Phys. Met. Metallogr.*, 2018, vol. 119, no. 5, pp. 477–481.
<https://doi.org/10.1134/S0031918X18050046>
 21. Bashev, V.F. and Kushnerev, A.I., Structure and properties of cast and splat-quenched high-entropy Al–Cu–Fe–Ni–Si alloys, *Phys. Met. Metallogr.*, 2017, vol. 118, no. 1, pp. 39–47.
<https://doi.org/10.1134/S0031918X16100033>
 22. Shaisultanov, D.G., Stepanov, N.D., Salishchev, G.A., and Tikhonovsky, M.A., Effect of heat treatment on the structure and hardness of high-entropy alloys Co–Cr–Fe–Ni–Mn–V_x ($x = 0.25, 0.5, 0.75, 1$), *Phys. Met. Metallogr.*, 2017, vol. 118, no. 6, pp. 579–590.
<https://doi.org/10.1134/S0031918X17060084>
 23. Meshkov, E.A., Novoselov, I.I., Yanilkin, A.V., Rogozhkin, S.V., Nikitin, A.A., Khomich, A.A., Shutov, A.S., Tarasov, B.A., Danilov, S.E., and Arbutov, V.L., Experimental and theoretical study of the atomic structure evolution of high-entropy alloys based on Fe, Cr, Ni, Mn, and Co upon thermal and radiation aging, *Phys. Solid State*, 2020, vol. 62, no. 3, pp. 389–400.
<https://doi.org/10.1134/S1063783420030130>
 24. Kireeva, I.V., Chumlyakov, Yu.I., Pobedennaya, Z.V., Vyrodova, A.V., Saraeva, A.A., Bessonova, I.G., Kuksgauzen, I.V., and Kuksgauzen, D.A., Temperature and orientation dependence of the mechanical properties of Al_{0.3}CoCrFeNi high-entropy alloy single crystals hardened by non-coherent β -phase particles, *Russ. Phys. J.*, 2020, vol. 63, no. 1, pp. 134–141.
<https://doi.org/10.1007/s11182-020-02012-8>
 25. Ma, Y., Peng, G.J., Wen, D.H., and Zhang, T.H., Nanoindentation creep behavior in a CoCrFeCuNi high-entropy alloys film with two different structure states, *Mater. Sci. Eng., A*, 2015, vol. 621, pp. 111–117.
<https://doi.org/10.1016/j.msea.2014.10.065>
 26. Wang, L.M., Chen, G.G., Yeh, J.W., and Ke, S.T., The microstructure and strengthening mechanism of thermal spray coating Ni_xCo_{0.6}Fe_{0.2}Cr_ySi_zAlTi_{0.2} high-entropy alloys, *Mater. Chem. Phys.*, 2011, vol. 126, no. 3, pp. 880–885.
<https://doi.org/10.1016/j.matchemphys.2010.12.022>
 27. Zhang, H., Wu, W., He, Y., Li, M., and Guo, S., Formation of core-shell structure in high-entropy alloy coating by laser cladding, *Appl. Surf. Sci.*, 2015, vol. 363, pp. 543–547.
<https://doi.org/10.1016/j.apsusc.2015.12.059>
 28. Gao, W.Y., Chang, C., Li, G., Xue, Y., Wang, J., Zhang, Z., and Lin, X., Study on the laser cladding of FeCrNi coating, *Optik*, 2019, vol. 178, pp. 950–957.
<https://doi.org/10.1016/j.ijleo.2018.10.062>
 29. Rong, Z., Wang, C., Wang, Y., Dong, M., You, Y., Wang, J., Liu, H., Liu, J., Wang, Y., and Zhu, Z., Microstructure and properties of FeCoNiCr_x ($x = \text{Mn, Al}$) high-entropy alloys, *J. Alloys Compd.*, 2022, vol. 921, p. 166061.
<https://doi.org/10.1016/j.jallcom.2022.166061>
 30. Chang, S.-Y., Lin, S.-Y., Huang, Y.-C., and Wu, C.-L., Mechanical properties, deformation behaviors and interface adhesion of (AlCrTaTiZr)_{N_x} multi-component coatings, *Surf. Coat. Technol.*, 2010, vol. 204, no. 20, pp. 3307–3314.
<https://doi.org/10.1016/j.surfcoat.2010.03.041>
 31. Shen, W.-J., Tsai, M.-H., Chang, Y.-S., and Yeh, J.-W., Effects of substrate bias on the structure and mechanical properties of (Al_{1.5}CrNb_{0.5}Si_{0.5}Ti)_{N_x} coatings, *Thin Solid Films*, 2012, vol. 520, no. 19, pp. 6183–6188.
<https://doi.org/10.1016/j.tsf.2012.06.002>
 32. Braic, V., Vladescu, A., Balaceanu, M., Luculescu, C.R., and Braic, M., Nanostructured multi-element (TiZrNbHfTa)_N and (TiZrNbHfTa)_C hard coatings, *Surf. Coat. Technol.*, 2012, vol. 211, pp. 117–121.
<https://doi.org/10.1016/j.surfcoat.2011.09.033>
 33. Lin, M.-I., Tsai, M.-H., Shen, W.-J., and Yeh, J.-W., Evolution of structure and properties of multi-component (AlCrTaTiZr)_{O_x} films, *Thin Solid Films*, 2010, vol. 518, no. 10, pp. 2732–2737.
<https://doi.org/10.1016/j.tsf.2009.10.142>
 34. Zhao, Y., Zhang, J., Wang, Y., Wu, K., Liu, G., and Sun, J., Size-dependent mechanical properties and deformation mechanisms in Cu/NbMoTaW nanolaminates, *Sci. China Mater.*, 2020, vol. 63, no. 3, pp. 444–452.
<https://doi.org/10.1007/s40843-019-1195-7>
 35. Cao, Z.H., Ma, Y.J., Cai, Y.P., Wang, G.J., and Meng, X.K., High strength dual-phase high entropy alloys with a tunable nanolayer thickness, *Scr. Mater.*, 2019, vol. 173, pp. 149–153.
<https://doi.org/10.1016/j.scriptamat.2019.08.018>
 36. Xu, H., Zang, J., Yuan, Y., Zhou, Y., Tian, P., and Wang, Y., In-situ assembly from graphene encapsulated CoCrFeMnNi high-entropy alloy nanoparticles for improvement corrosion resistance and mechanical properties in metal matrix composites, *J. Alloys Compd.*, 2019, vol. 811, p. 152082.
<https://doi.org/10.1016/j.jallcom.2019.152082>

37. Wang, Y., Kuang, S., Yu, X., Wang, L., and Huang, W., Tribo-mechanical properties CrNbTiMoZr high-entropy alloy films synthesized by direct magnetron sputtering, *Surf. Coat. Technol.*, 2020, vol. 403, p. 126374. <https://doi.org/10.1016/j.surfcoat.2020.126374>
38. Zhao, S., He, L., Fan, X., Liu, C., Long, J., Wang, L., Chang, H., Wang, J., and Zhang, W., Microstructure and chloride corrosion property of nanocrystalline Al-TiCrNiNa high entropy alloy coating on X80 pipeline steel, *Surf. Coat. Technol.*, 2019, vol. 375, pp. 215–220. <https://doi.org/10.1016/j.surfcoat.2019.07.033>
39. Wu, H., Zhang, S., Wang, Z.Y., Zhang, C.H., Chen, H.T., and Chen, J., New studies on wear and corrosion behavior of laser cladding FeNiCoCrMo_x high-entropy alloy coating: the role of Mo, *Int. J. Refract. Met. Hard Mater.*, 2022, vol. 102, p. 105721. <https://doi.org/10.1016/j.ijrmhm.2021.105721>
40. Ye, F., Jiao, Z., Yan, S., Guo, L., Feng, L., and Yu, J., Microbeam plasma arc remanufacturing: effects of Al on microstructure, wear resistance, corrosion resistance and high temperature oxidation resistance of Al_xCoCrFeMnNi high-entropy alloy cladding layer, *Vacuum*, 2020, vol. 174, p. 109178. <https://doi.org/10.1016/j.vacuum.2020.109178>
41. Zhang, G., Liu, H., Tian, X., Chen, P., Yang, H., and Hao, J., Microstructure and properties of AlCoCrFeNiSi high-entropy alloy coating on AISI 304 stainless steel by laser cladding, *J. Mater. Eng. Perform.*, 2020, vol. 29, pp. 278–288. <https://doi.org/10.1007/s11665-020-04586-3>
42. Liu, H., Zhang, T., Sum, S., Zhang, G., Tian, X., and Chen, P., Microstructure and dislocation density of AlCoCrFeNiSi_x high-entropy alloy coatings by laser cladding, *Mater. Lett.*, 2021, vol. 283, p. 128746. <https://doi.org/10.1016/j.matlet.2020.128746>
43. Ye, Q., Feng, K., Li, Z., Lu, F., Li, R., Huang, J., and Wu, Y., Microstructure and corrosion properties of CrMnFeCoNi high-entropy alloy coating, *Appl. Surf. Sci.*, 2017, vol. 396, pp. 1420–1426. <https://doi.org/10.1016/j.apsusc.2016.11.176>
44. Jiang, H., Han, K., Li, D., and Cao, Z., Synthesis and characterization of AlCo–CrFeNiNb_x high entropy alloy coatings by laser cladding, *Crystals*, 2019, vol. 9, no. 1, p. 56. <https://doi.org/10.3390/cryst9010056>
45. Liu, S.S., Zhang, M., Zhao, G., Wang, X.H., and Wang, J.F., Microstructure and properties of ceramic particle reinforced FeCoNiCrMnTi high entropy alloy laser cladding coating, *Intermetallics*, 2022, vol. 140, p. 107402. <https://doi.org/10.1016/j.intermet.2021.107402>
46. Zhong, M., Wang, D., He, L., Ye, X., Ouyang, W., Xu, Z., Zhang, W., and Zhou, X., Microstructure and elevated temperature wear behavior of laser cladding NiMnFeCrAl high entropy alloy coating, *Opt. Laser Technol.*, 2022, vol. 149, p. 107845. <https://doi.org/10.1016/j.optlastec.2022.107845>
47. Zhang, P., Xu, Z., Yao, Z., Liu, Y., Lin, S., He, M., Lu, S., and Wu, X., A high corrosion resistant high-entropy alloys (HEAs) coatings with single BCC solid solution structure by laser remelting, *Mater. Lett.*, 2022, vol. 324, p. 132728. <https://doi.org/10.1016/j.matlet.2022.132728>
48. Liu, H., Li, X., Liu, J., Gao, W., Du, X., and Hao, J., Microstructural evolution and properties of dual-layer CoCrFeMnTi_{0.2} high-entropy alloy coating fabricated by laser cladding, *Opt. Laser Technol.*, 2021, vol. 134, p. 106646. <https://doi.org/10.1016/j.optlastec.2020.106646>
49. Zhang, Y., Han, T., Xiao, M., and Shen, Y., Effect of Nb content on microstructure and properties of laser cladding FeNiCoCrTi_{0.5}Nb_x high-entropy alloy coating, *Optik*, 2019, vol. 198, p. 163316. <https://doi.org/10.1016/j.ijleo.2019.163316>
50. Liu, S.S., Zhang, M., Zhao, G.L., Wang, X.H., and Wang, J.F., Microstructure and properties of ceramic particle reinforced FeCoNiCrMnTi high entropy alloy laser cladding coating, *Intermetallics*, 2022, vol. 140, p. 107402. <https://doi.org/10.1016/j.intermet.2021.107402>
51. Jiang, X.J., Wang, S.Z., Fu, H., Chen, G.Y., Ran, Q.X., Wang, S.Q., and Han, R.H., A novel high entropy alloy coating on Ti–6Al–4V substrate by laser cladding, *Mater. Lett.*, 2022, vol. 308, part B, p. 131131. <https://doi.org/10.1016/j.matlet.2021.131131>
52. Deng C., Wang C., Chai L., Wang T., and Luo J. Mechanical and chemical properties of CoCrFeNiMo 0,2 high entropy alloy coating fabricated on Ti–6Al–4V by laser cladding, *Intermetallics*, 2022, vol. 144, p. 107504. <https://doi.org/10.1016/j.intermet.2022.107504>
53. Bingyuan, H., Shaoyi, B., Wenbo, D., Weixing, H., Xue, Y., Fang-Fang, C., Jiajie, C., Xianghan, G., and Sheng, Z., Laser irradiation induced dynamically recrystallized microstructure and properties of super-sonic particle deposited Ni–Fe–Cr–Nb–Ti–Al high entropy alloy coating, *Mater. Charact.*, 2022, vol. 183, p. 111600. <https://doi.org/10.1016/j.matchar.2021.111600>
54. Guo, J., Goh, M., Zhu, Z., Lee, X., Nai, M.L.S., and Wei, J., On the machining of selective laser melting CoCrFeMnNi high entropy alloy, *Mater. Des.*, 2018, vol. 153, pp. 211–220. <https://doi.org/10.1016/j.matdes.2018.05.012>
55. Lindner, T., Lobel, M., Sattler, B., and Lampke, T., Surface hardening of FCC phase high entropy alloy system by powder pack boriding, *Surf. Coat. Technol.*, 2019, vol. 371, pp. 389–394. <https://doi.org/10.1016/j.surfcoat.2018.10.017>
56. Erdogan, A., Günen, A., Gök, M.S., and Zeytin, S., Microstructure and mechanical properties of borided CoCrFeNiAl_{0.25}Ti_{0.5} high entropy alloy produced by powder metallurgy, *Vacuum*, 2021, vol. 183, p. 109820. <https://doi.org/10.1016/j.vacuum.2020.109820>
57. Ivanov, Yu.F., Gromov, V.E., Zagulyaev, D.V., Kononov, S.V., Rubannikova, Yu.A., and Semin, A.P., Prospects for the application of surface treatment of alloys by electron beams in state of the art technologies, *Prog. Phys. Met.*, 2020, vol. 21, no. 3, pp. 345–362. <https://doi.org/10.15407/ufm.21.03.345>
58. Gromov, V.E., Kononov, S.V., Ivanov, Yu.F., Osintsev, K.A., Shlyarova, Yu.A., and Semin, A.P., *Struktura i svoystva vysokoentropiinykh splavov* (Structure and Properties of High-Entropy Alloys), Novokuznetsk: Sib. Gos. Ind. Univ., 2022.
59. Gromov, V.E., Kononov, S.V., Ivanov, Yu.F., Shlyarova, Yu.A., Vorobyov, S.V., and Semin, A.P., Structure and properties of the CrMnFeCoNi high entropy alloy

- irradiated with a pulsed electron beam, *J. Mater. Res. Technol.*, 2022, vol. 19, pp. 4258–4269.
<https://doi.org/10.1016/j.jmrt.2022.06.108>
60. Osintsev, K.A., Gromov, V.E., Ivanov, Yu.F., Kononov, S.V., Panchenko, I.A., and Vorobyov, S.V., Evolution of structure in AlCoCrFeNi highentropy alloy irradiated by pulsed electron beam, *Metals*, 2021, vol. 11, no. 8, p. 1228.
<https://doi.org/10.3390/met11081228>
61. Gromov V.E., Ivanov, Yu.F., Osintsev, K.A., Vorob'ev, S.V., Panchenko, I.A., Fractography of fracture surface of CrMnFeCoNi highentropy alloy after electronbeam processing, *Izv. Vyssh. Uchebn. Zaved., Chern. Metall.*, 2022, vol. 65, no. 6, pp. 427–433.
<https://doi.org/10.17073/0368-0797-2022-6-427-433>
62. Gromov, V.E., Shlyarova, Yu.A., Ivanov, Yu.F., Kononov, S.V., and Vorob'ev, S.V., Effect of electron beam treatment on the fracture behavior of high-entropy Cr–Mn–Fe–Co–Ni alloy, *Met. Sci. Heat Treat.*, 2022, no. 5, pp. 276–280.
<https://doi.org/10.1007/s11041-022-00800-2>
63. Gromov, V.E., Ivanov, Yu.F., Kononov, S.V., and Osintsev, K.A., Effect of electron beam treatment on the structure and properties of AlCoCrFeNi highentropy alloy, *CIS Iron Steel Rev.*, 2021, vol. 22, pp. 72–76.
<https://doi.org/10.17580/cisisr.2021.02.13>
64. Gromov, V.E., Ivanov, Yu.F., Shlyarova, Yu.A., Kononov, S.V., Vorob'ev, S.V., and Kirillova, A.V., Modification of structure and properties of highentropy CrMnFeCoNi alloy by pulsed electron beam, *Probl. Chern. Metall. Materialoved.*, 2022, no. 1, pp. 65–76.
https://doi.org/10.54826/19979258_2022_1_65

Translated by M. Astrov